Journal of Applied Physics ARTICLE scitation.org/journal/jap

Deep trap analysis in green light emitting diodes: Problems and solutions

Cite as: J. Appl. Phys. **125**, 215701 (2019); doi: 10.1063/1.5093723
Submitted: 24 February 2019 · Accepted: 14 May 2019 ·
Published Online: 3 June 2019

A. Y. Polyakov,[1] N. M. Shmidt,[2] N. B. Smirnov,[1] I. V. Shchemerov,[1] E. I. Shabunina,[2] N. A. Tal'nishnih,[3] In-Hwan Lee,[4] L. A. Alexanyan,[1] S. A. Tarelkin,[1,5] and S. J. Pearton[6,a)]

AFFILIATIONS

[1]National University of Science and Technology MISiS, Moscow 194017, Russia
[2]Ioffe Physico-Technical Institute, 26 Polytekhnicheskaya Str., St. Petersburg 194021, Russia
[3]Submicron Heterostructures for Microelectronics Research and Engineering Center, St. Petersburg 194021, Russia
[4]Department of Materials Science and Engineering, Korea University, Seoul 02841, South Korea
[5]Technological Institute for Superhard and Novel Carbon Materials, 7 Centralnaya St., Troitsk, Moscow 142190, Russia
[6]Department of Materials Science and Engineering, University of Florida, Gainesville, Florida 32611, USA

[a)]**Author to whom correspondence should be addressed:** spear@mse.ufl.edu

ABSTRACT

Some green light emitting diodes (LEDs) based on GaN/InGaN multiquantum-well (MQW) structures exhibit strong frequency and temperature dependence of capacitance and prominent changes in capacitance–voltage profiles with temperature that make it difficult to obtain reliable deep level transient spectroscopy (DLTS) measurements. DLTS performed at low probing signal frequency and with constant capacitance between the measurements by controlling applied bias mitigates these issues. This allows measurement of deep electron and hole traps in specific quantum wells (QWs) in the MQW structure. The dominant electron and hole traps detected have levels near E_{c-} (0.45–0.5) eV and E_{v+} (0.6–0.63) eV. Their density increases significantly after aging for a long period (2120 h) at high driving current and elevated temperature. The reason for the observed anomalies in DLTS spectra of these green LEDs is the high density of states in the QWs with activation energies near 0.08, 0.12–0.14, and 0.3 eV, detected in admittance spectra, and, for the 0.08 eV and 0.3 eV, these states are likely related to defects.

I. INTRODUCTION

Light emitting diodes (LEDs) based on GaN/InGaN multiquantum-well (MQW) structures are key components of modern general lighting systems, displays, indicators, scientific research instrumentation, and various detecting systems.[1–3] Their performance is influenced by the presence of deep traps in quantum wells (QWs) and quantum barriers (QBs), causing enhanced nonradiative recombination in the active region for the former and a decrease in injection efficiency for the latter.[4] Together with the presence of local variations of the QW composition, these factors largely determine the peak internal quantum efficiency of GaN-based LEDs.[4–7] Deep traps with levels not much deeper than ~1 eV can be measured by standard deep level transient spectroscopy (DLTS),[8] while deeper traps can be probed by photocapacitance and deep level optical spectroscopy (DLOS).[9] The locations of the traps can be obtained by varying biasing/pulsing conditions in DLTS.[10]

Problems can be encountered due to freeze out of Mg acceptors causing a pronounced decrease of capacitance at temperatures below ~200 K. This may produce false peaks in DLTS and shift the apparent position of the QWs with respect to the p–n junction plane as determined from C–V profiles at different frequencies.[11,12] The MQW region should preferably be located inside the space charge region (SCR) of the diode at 0 V bias. This means that in order to selectively probe deep traps in the QWs, one has to operate at biases close to zero or slightly positive.[11] A redeeming factor is the high built-in voltage in GaN-based LEDs and the presence of a strong polarization field that can separate charge carriers in the SCR even in the absence of an external bias.[11] The impact of these factors adversely affecting the ability to detect deep traps in

the MQW region can be alleviated for many types of LEDs operating in the blue, near-UV, and green spectral regions by decreasing the probing frequency in DLTS measurements and by appropriate choice of biasing and pulsing conditions.[10–12] However, quantized electron states in QWs can be quite deep in the case of green MQW GaN/InGaN LEDs (some tenths of an electron volt). The electron exchange time of these states with the conduction band can be long so these states are not fully emptied during C–V profiling sweeps or during pulsing cycles in DLTS.

In green LEDs, the density of interface states can be also significant.[3,13,14] These can contribute to frequency and temperature delays in DLTS and admittance spectroscopy. This results in a temperature dependence of the voltage necessary to empty the states. Consequently, capacitance relaxations in DLTS obtained at fixed quiescent bias and fixed bias pulse values will be taken at different places in the MQW region for different temperatures, and the spectra will be misleading. In this paper, we demonstrate the presence of these effects in commercial green LEDs and detail procedures to selectively probe deep traps in different QWs of the structure.

II. EXPERIMENTAL

The green LEDs were commercial chips with an area of $1 \times 1\ mm^2$. The nominal peak wavelength in electroluminescence (EL) was 530 nm, and the peak external quantum efficiency (EQE) of EL was ~14%. According to the manufacturer, the LED structure was grown on patterned sapphire substrates and consisted of Si doped n-type GaN (5 μm), strain-relieving GaN/InGaN superlattice (thickness 250 nm), 8 InGaN QWs (thickness 3.5 nm) with undoped GaN barriers (12 nm), and 160-nm-thick p-GaN (Mg) emitter. The samples were characterized by current–voltage (I–V) at different temperatures, capacitance vs frequency (C–f), capacitance vs voltage (C–V), admittance spectra,[15] and DLTS with electrical or optical (ODLTS) injection.[8,16] These were carried out from 80 to 400 K.[10–12] A feature of our DLTS setup is that it allows performing measurements at probing frequencies from 10 kHz to 1 MHz,[16] as opposed to the fixed probing frequency (usually 1 MHz) in commercial spectrometers. This allows alleviation of the problems related to Mg freeze-out in p-GaN, leading to a strong decrease of capacitance at a temperature below ~200 K[10–12] and also to decrease the impact of capacitance changes owing to frequency dispersion of response of the charge determining the space charge region (SCR) width at different temperatures. Another important feature is the ability to maintain constant chosen capacitance between the DLTS relaxation curve measurements by varying the bias applied to the diode. Finally, we also measured the spectral dependence of the external quantum efficiency of EL and the effect of operation for 2120 h at high driving current (600 mA) at 80°C and looked at changes in deep trap spectra introduced by this aging test.

III. RESULTS AND DISCUSSION

The nature of the measurement artifacts is illustrated by Figs. 1 and 2. Figure 1(a) displays the frequency (f) dependence of the diode capacitance (C) at 0 V bias as measured at several temperatures from 218 to 400 K. There are three steps in capacitance, corresponding to peaks in frequency dependences of AC

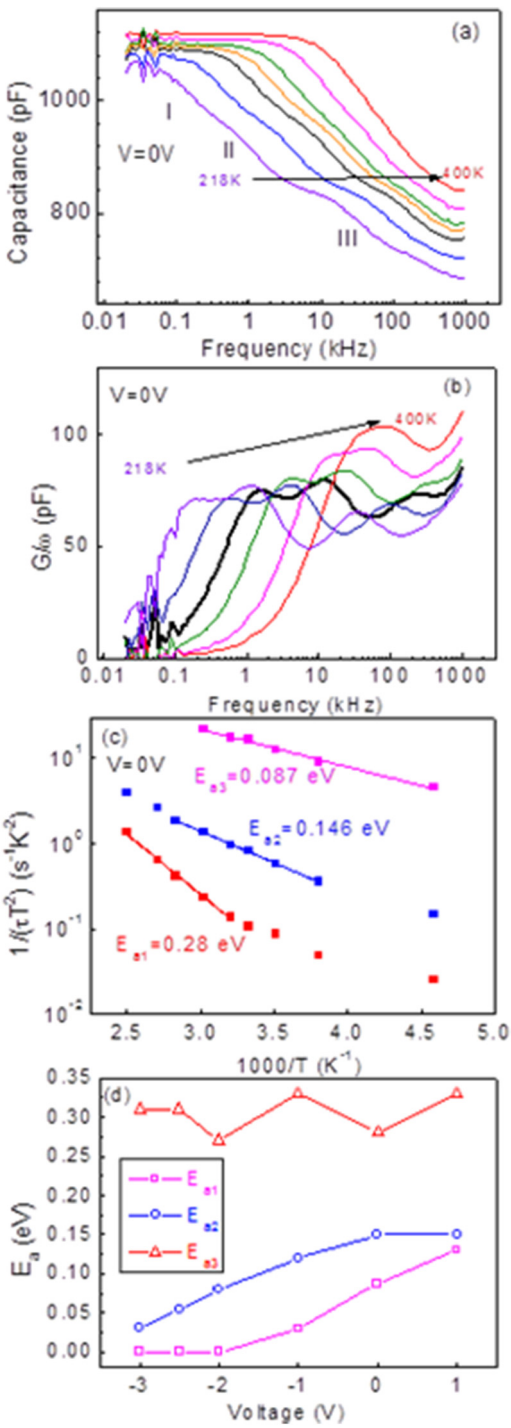

FIG. 1. (a) Capacitance at 0 V dependence on frequency from 218 K to 400 K; (b) G/ω frequency dependence for the same temperature range ($\omega = 2\pi f$); (c) Arrhenius plots $\ln(1/(\tau T^2))$ vs 1000/T for the three processes detected in G/ω vs temperature dependences, $\tau = 1/\omega$; and (d) the dependence of the three activation energies on applied voltage.

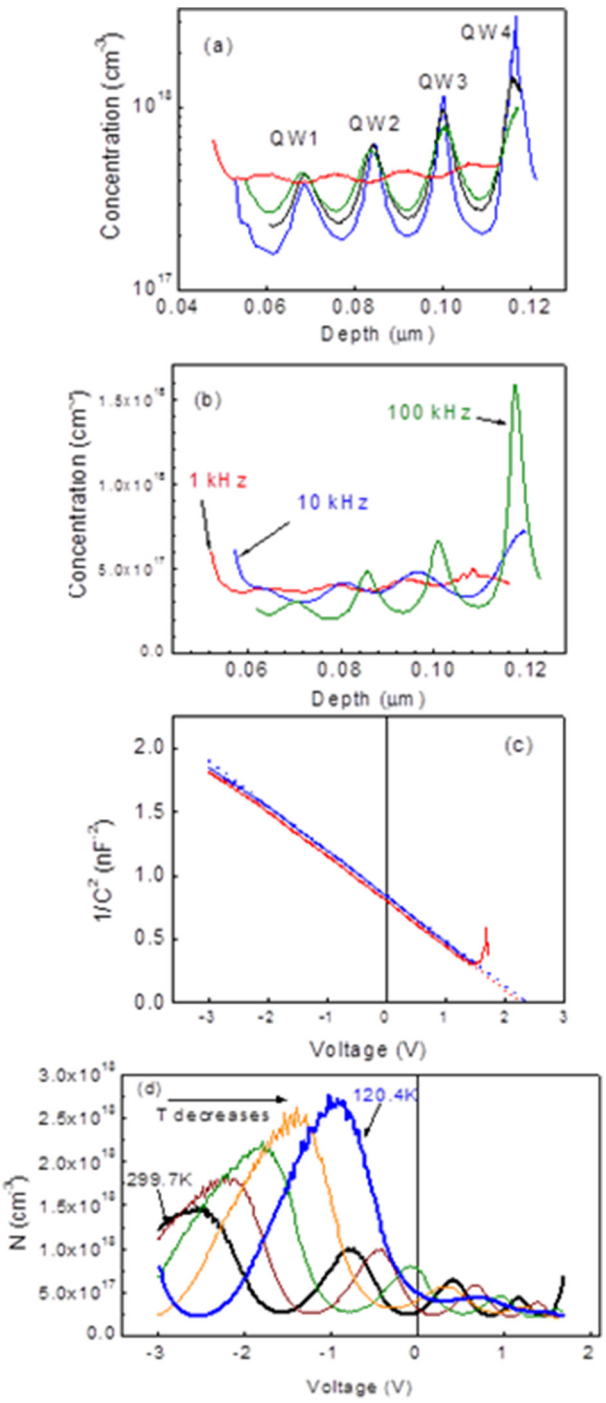

FIG. 2. (a) Concentration profiles from C–V measurements at 0.3 kHz at 83 K (blue line), at 10 kHz, 290 K (black line), at 1 kHz, 290 K (olive line), and at 10 kHz, 400 K (red line); (b) concentration profiles measured at 400 K at 1 kHz (red line), 10 kHz (blue line), 100 kHz (olive line); (c) $1/C^2$ vs voltage at 400 K obtained at 3 kHz (red line) or 10 kHz (blue line); and (d) concentration vs voltage profiles obtained at 10 kHz for different temperatures.

conductance G in Fig. 1(b) (G value is normalized by the angular frequency $\omega = 2\pi f$[15]). The standard admittance spectroscopy analysis allows calculating the activation energies corresponding to respective processes responsible for each step/peak, Ea_1, Ea_2, and Ea_3, as determined from the Arrhenius plots of $\ln(1/(\tau T_M^2))$ vs $1000/T_M$ (τ is $\tau = 1/\omega$, and T_M is the temperature of the peak/step). The resulting plots are depicted in Fig. 2(c) for zero bias. The corresponding values of the activation energies for steps I, II, and III marked in Fig. 1(a) were $Ea_1 = 0.087$ eV, $Ea_2 = 0.15$ eV, and $Ea_3 = 0.28$ eV (the leveling-off of the E_{a2} and E_{a3} Arrhenius plots at low temperatures is due to the onset of tunneling). Increasing the reverse bias decreased the activation energies Ea_1 and E_{a2} (at high reverse biases, E_{a1} centers could no longer be seen) but had little effect on Ea_3 [Fig. 1(d)].

From Fig. 1, it is clear that, even at room temperature, meaningful C–V profiling experiments and, consequently, DLTS measurements must be performed at frequencies <10 kHz. This is not a result of failure to prepare good quality Ohmic contacts because in that case, one expects to see one step in C–f and not three distinct activation energies in admittance spectra. In addition, the high-frequency capacitance should be the geometrical capacitance of the structure. Instead, one is dealing with the delayed response of three types of electronic states that determine the width of the space charge region.

When calculating the spatial distribution of charge N in the SCR from $1/C^2$–V using the standard depletion approximation,[17] one observes 4 peaks approximately corresponding to the positions of the 4 quantum wells that could be probed by C–V profiling [Fig. 2(a)]. From the concentration profiles in Fig. 2, the overall width of the MQW region in our LEDs is ~0.12 μm, the width of the InGaN QW is ~3 nm, and the width of the QW + QB is ~15 nm, which is in agreement with the LED design description. The four deepest lying QWs of the total number of 8 could be probed by C–V profiling—two were outside the SCR at 0 V bias and two were inside. The origin of the peaks is due to the pinning of the space charge region width dependence on applied voltage at approximately the same position until the charge of the quantized states of the QW and/or of interface states at the QW/QB boundary is depleted. If this C–V profiling is done at a fixed temperature at different frequencies, the apparent position of the QWs will be different because of the C–f dependences in Fig. 1. This is illustrated in Fig. 2(a). The 290 K profiles measured at 1 kHz (olive line) and 10 kHz (black line) are shifted with respect to each other: the higher the frequency, the deeper the peaks in profiles corresponding to QWs. For 83 K profiling at 10 kHz, the peaks are further shifted to higher apparent depth positions. However, if the measurements at this low temperature are performed at a very low frequency of 0.3 kHz (blue line), the room temperature profile and the 83 K profile become similar. Measurement of profiles at 10 kHz at the high temperature of 400 K further shifts the apparent peak positions closer to the p–n junction plane (red line). This is the consequence of the strong frequency dispersion of capacitance that requires correct profiling experiments to be done at very low frequencies. The ability to correctly reveal the details of the concentration profile is dependent on the charge carriers not being able to escape from the QWs when the probing frequency is so low that it is comparable to the emission rate of electrons from the states in

the QW. Otherwise, the apparent concentration of charge in the QW as determined from C–V profiling will decrease with decreasing measurement frequency, as illustrated by Fig. 2(b) for measurements at 400 K. At low frequency, there is virtually no localization of charge in the QWs, and the $1/C^2$–V dependence yields a straight line with slope equal to the average concentration in the MQW region and voltage offset corresponding to the effective band bending [respectively, 4.3×10^{17} cm^{-3} and 2.3 V in Fig. 2(c)]. The data in Figs. 2(a)–2(c) suggest that profiling measurements have to be performed at very low frequencies at lower temperatures, but at high temperatures, the frequency should be increased to preserve the charge localization in the QWs and correct magnitude of charge stored in the QWs. In DLTS, one has to perform the measurements at a fixed frequency. The lower the measurement frequency, the better one can fix the position in the structure where the deep traps are being probed. In our DLTS setup, the lowest frequency is 10 kHz. This frequency is still high in the above explained sense for all temperatures below room temperature. The consequence is the voltage corresponding to the chosen QW will be different for measurements at different temperatures. This is illustrated by Fig. 2(d). The voltage corresponding to a certain QW systematically shifts to lower values and the apparent charge concentration stored in the QW increases with decreasing temperature.

Therefore, if one sets the steady-state bias at, say, −1.5 V and pulses it to −0.5 V at 120.4 K, one is probing the 4th QW, with corresponding depth values obtained from measured capacitance. However, for 299.7 K, this set of bias/pulsing voltages will be probing the 3rd QW. The strong changes of capacitance from one temperature point where the capacitance relaxation curve is monitored to the other temperature point can destroy coherence in the spectra and cause the appearance of DLTS peaks whose temperature does not shift with changing t_1/t_2 time windows settings and even give rise to false hole-traplike peaks. This occurred for our LEDs, as illustrated by DLTS and ODLTS spectra in Figs. 3(a) and 3(b). This is similar to DLTS probing of deep centers in GaN-based high electron mobility transistors whose threshold voltage strongly changes with temperature because of electron trapping/detrapping in the barrier.[18] The best remedy is to employ the constant capacitance DLTS mode in which the spectra are obtained from the applied voltage relaxation curves.[17]

Another option is keeping capacitance constant in between the capacitance relaxation measurements, by continuously adjusting the applied voltage via controlled feedback capacitance measurement and regulation. The different QWs of the MQW region can be probed, with the QWs nearest the p–n junction being of greatest interest. There are limitations in the LEDs tested, in that these QWs are located inside the SCR of the diode at zero bias and can be probed only with quiescent positive voltage and a positive voltage pulse. These conditions are conducive to recharging of hole traps but do not provide good sensitivity for electron traps. Conversely, for QWs outside the SCR at zero bias, one can easily probe electron traps, but not hole traps using electrical pulse injection. For the latter, the remedy is using optical excitation resonant with the InGaN QW bandgap. For the former, there is no general fix, but if excitation with photons with energy below the InGaN

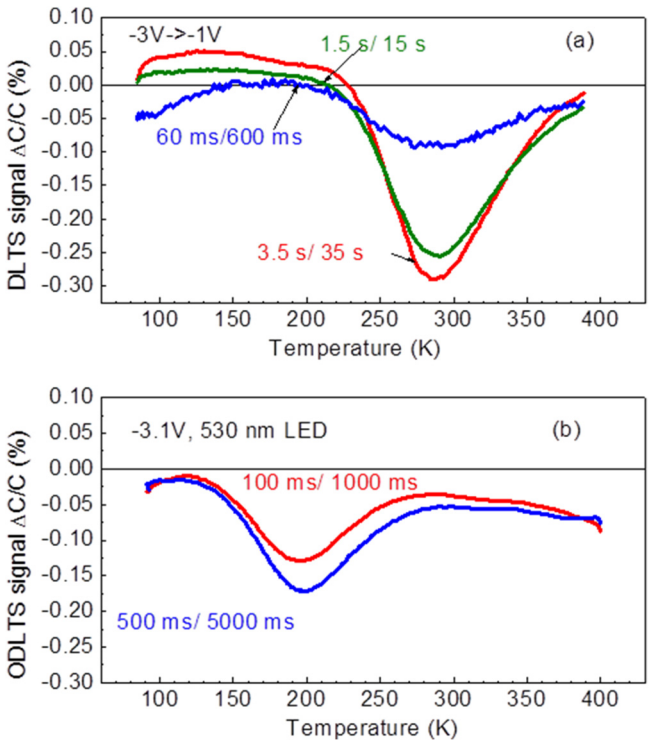

FIG. 3. (a) DLTS spectra with three different t1 and t2 values (shown near respective curves) with bias −3 V pulsed for 3 s to −1 V and (b) ODLTS spectra taken with bias −3 V, 2 time windows (shown near respective curves) with 530-nm-wavelength LED excitation (pulse 5 s-long), measurements at 10 kHz in both cases.

bandgap can recharge empty electron traps, they might appear in the spectra. For QWs observable only with applied forward voltage, the ability to obtain DLTS/ODLTS spectra depends on the efficiency of detrapped charge carrier collection by the p–n junction and decreases as the built-in voltage is compensated by the applied forward voltage.

There still remains some error coming from the reference capacitance C changing during the capacitance relaxation measurement. The solution is to keep temperature constant for each relaxation measurement, but this makes accurate measurements time consuming. The compromise is to set the temperature sweep reasonably slow. The quality of the spectra measurements can be further improved by independently measuring the derivative of the temperature dependence of capacitance dC/dT, as a function of temperature at a fixed slow temperature ramp, convert the dC/dT at the temperature of interest into the time derivative at a specified temperature, dC/dt(T), and introducing an additional correction by subtracting the $\Delta t \times P \times dC/dt$ line from the experimental capacitance relaxation curve. One can then calculate the corrected DLTS signal $\Delta C = C(t_1) - C(t_2)$ (Δt is the time step used to digitize the capacitance relaxation curve, P the number of points on the digitized relaxation curve, and t_1 and t_2 the time windows chosen to obtain the

DLTS spectrum[16]). We found with a temperature ramp of ~2 K/min and our typical relaxation times, this correction is minor.

Based on capacitance–voltage profiling, the capacitance at 10 kHz was kept constant at 660 pF, corresponding to the deepest 4th quantum well, QW4 (starting voltage at a low temperature of −1 V decreasing to ~−2.5 V as temperature increased), 755 pF for the second deepest 3rd QW3 (starting voltage 0.3 V decreasing to ~−0.8 V), 880 pF for the 2nd QW2 (inside the SCR at all temperatures), and 1060 pF for the 1st QW1 (inside the SCR at all temperatures). For these two latter QWs, the spectra were only measured above ~200 K where the voltage corresponding to the QW peaks in concentration vs voltage plots was located below the forward voltage of 1.5 V. The forward bias pulse was kept constant at +0.7 V above the quiescent bias.

The results are depicted for QW1 and QW4 in Fig. 4. The convention in the figure is that electron-traplike peaks (capacitance increases with time after pulse) have a positive sign, while hole-traplike peaks (capacitance decreases with time) are negative. DLTS spectra of QW1 were collected with voltage pulsing to high positive values bound to inject holes. Consequently, these spectra were dominated by a prominent hole trap peak, peak B [Fig. 4(a)]. For the lowermost QW4, on the contrary, deep electron traps could be easily probed without interference from the signal from hole traps. This could be done by pulsing from reverse voltage corresponding to the depletion of these QWs to lower the reverse voltage at which the edge of the SCR passes the QW. A weak signal due to electron traps A in QW4 thus detected can be seen in Fig. 4(b). Problems arise when trying to detect electron traps in the QWs lying deep inside the SCR at 0 V and only accessible for deep trap probing by the application of forward bias. Pulsing to higher forward bias in DLTS is bound to strongly favor the detection of hole traps. Deep electron traps in such QWs can still be detected in ODLTS spectra measured with subbandgap excitation that can fill electron traps in the upper half of the QW bandgap while not producing, under optimized conditions, the refilling of deep hole traps whose signal interferes with the electron trap signal. This has indeed been observed for QW1 where optical excitation with subbandgap light with the wavelength 660 nm revealed the presence of electron traps A as seen in Fig. 4(c). Hole traps in the QWs outside the SCR can be probed by ODLTS excited with photons having energy close to the bandgap of the InGaN QW. Even for quite low densities of probed traps [ΔC/C of (0.05–0.1) %], this approach allowed observation of electron and hole traps in specific regions.

Prolonged LED operation at high driving current and elevated temperature (2120 h, 600 mA, 80 °C) led to an increase in magnitude of all peaks (Fig. 5). Peak magnitudes could be compared for adjacent quantum wells [compare electron trap spectra for QW4 and QW3, and hole traps for QW1 and QW2 in Fig. 5(a)]. In Fig. 5(b), the hole trap spectra obtained with 530 nm wavelength excitation are compared for QW4 and QW1. The magnitudes of both A electron trap peaks and B hole trap peaks increase as one moves away from the p–n junction.

The hole trap B was found to be near E_{v^+}(0.6–0.63) eV (from the top of the valence band in the InGaN QW or at the GaN/InGaN interface), with hole capture cross section $\sigma_p = 10^{-16}$ cm^2. For electron traps A, the level was E_c–(0.45–0.5 eV), with electron

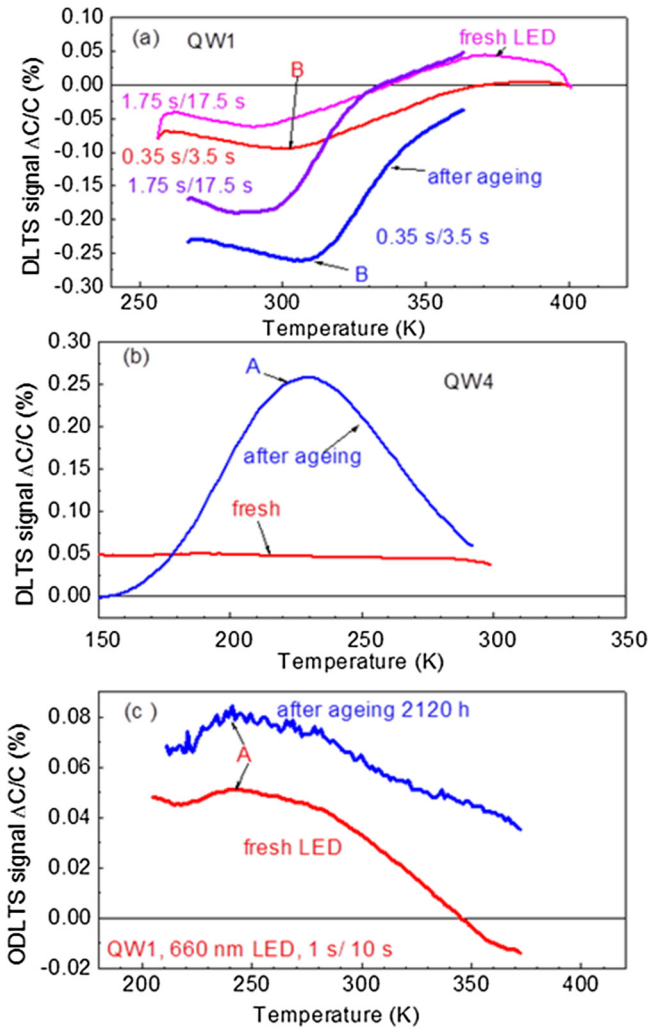

FIG. 4. (a) DLTS spectra for two time windows measured for QW1 before and after aging; (b) DLTS spectra for QW4 measured before and after aging; (c) ODLTS spectra for QW1 measured with below-bandgap 660 nm LED excitation showing the electron trap signal; the data shown before and after the aging test.

capture cross section $\sigma_n = (8.8–16) \times 10^{-17}$ cm^2. These traps are similar to electron traps ET4 and hole traps HT1 detected in green LEDs and reported to increase in concentration after electron irradiation,[19,20] similar to the effect we observe in our green LEDs after the aging test. We have not seen a decrease of EQE after prolonged operation for our LEDs, despite the increase of the signal of electron traps A and hole traps B. After the aging test, the peak EQE slightly increased from 14% to 18%. This is explained by the spectral dependence of EQE on forward voltage and from the peak EL wavelength dependence on forward voltage, as presented in Figs. 6(a) and 6(b). Figure 6(c) shows the EL intensity spectra taken before the aging test for different driving current values. Before the aging test, the wavelength at low voltages extended to 538 nm

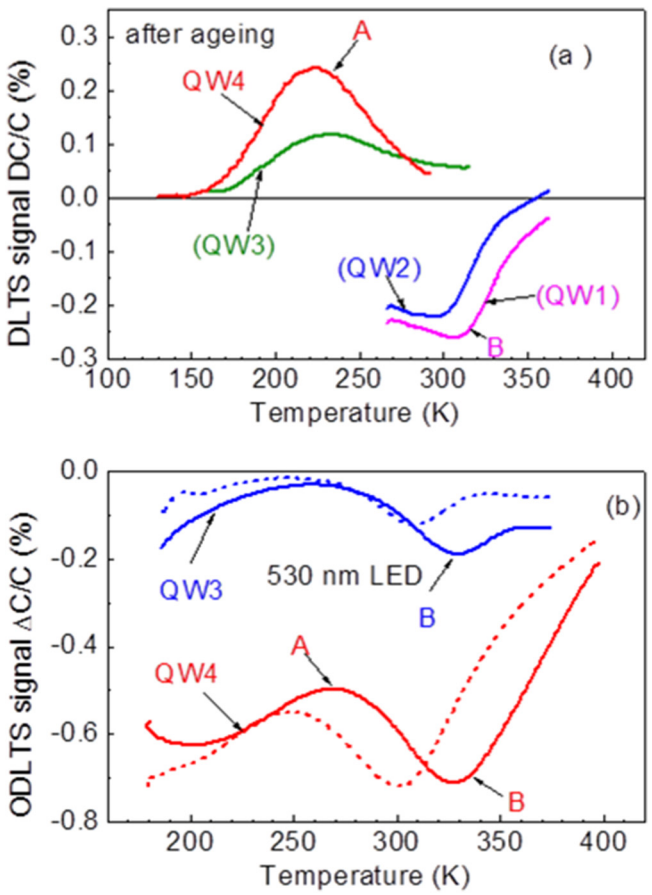

FIG. 5. (a) DLTS spectra for LED after aging for QW4 (red curve) and QW3 (olive curve) and the spectra for QW1 (magenta curve) and QW2 (blue curve) and (b) ODLTS after aging; 530 nm LED excitation; two time windows; measured for QW4 and QW3.

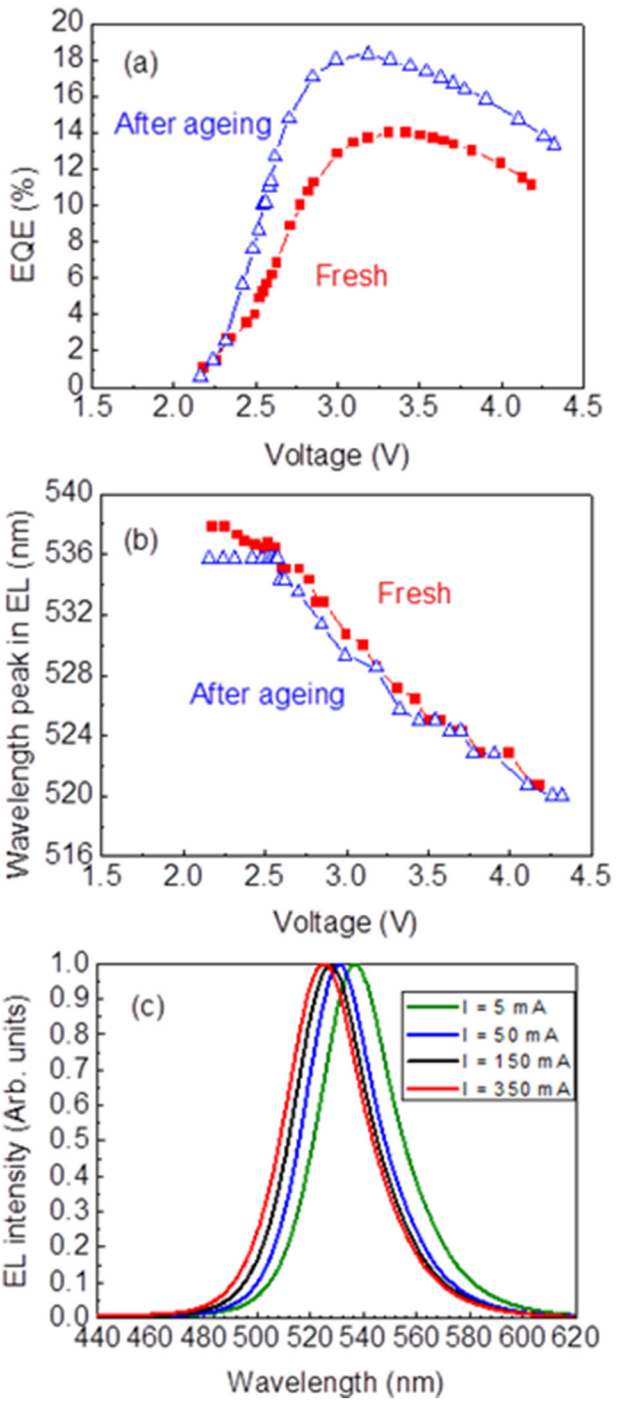

FIG. 6. (a) Dependence of EQE on forward voltage before (solid red squares) and after (blue open triangles) aging for 2120 h; (b) dependence of peak wavelength in EL normalized to the forward voltage before and after aging; (c) EL intensity spectra at different driving current values (5 mA—olive line, 50 mA—blue line, 150 mA—black line, 350 mA—red line) measured before the aging test; the intensities are normalized by the intensities in the peak.

[Fig. 6(a)] and had low EQE [Fig. 6(b)]. After the aging test, this low-efficiency, long-wavelength tail in EL was suppressed [Fig. 6(b)]. The EL emission spectrum in Fig. 6(c) is governed by the presence of In-rich regions in the QW (shifting the spectrum to longer wavelengths), possible local QW thickness variations (as, e.g., by V-pit defects),[21] and the magnitude of the quantum-confined-Stark-effect (QCSE),[22] whose operation shifts the spectrum to shorter wavelength with increasing current.

With well-organized In-rich regions, one expects radiative recombination to be dominated by these regions and the EL wavelength in the peak of EQE dependence on driving current to be close to the wavelength emitted by these In-rich regions. This is not the case in the studied LEDs, where the EQE of long-wavelength EL is low. This suggests that these regions are not well ordered and are characterized by low luminescence efficiency. The increase of EQE after aging, taken together with the decrease of the EL spectrum spread into the long-wavelength region, would imply a decrease of In composition in the region of fluctuations. There

could be an associated increase in defect density associated with In-rich conditions, such as In interstitials and Ga vacancies, in the surrounding regions of QWs. We suggest that the increase of electron traps A and hole traps B could be the result of such ordering of In-rich regions with the A traps corresponding to In interstitials and B traps to In or Ga vacancy complexes.

The absolute concentrations of traps detected in DLTS/ODLTS are also important. Normally, this is obtained by multiplying the peak amplitude $\Delta C/C$ by $2N$, where N is the local charge concentration determining the width of the space charge region.[8,17] However, experimentally measured N for quantum wells varies with frequency and temperature. This was obtained using the depletion approximation in which the change in capacitance during the capacitance sweep is attributed to the change of the width of the space charge region. For QWs, this is not the case exactly, since the charge changes because of changing population of the quantized levels in the QW. For III-nitrides, the situation is further aggravated by the necessity to account for the strong polarization fields adding to the band bending and to charge density in the QW depending on strain. Modeling of these states can be done by existing software packages that also allow calculation of the quasistatic capacitance but cannot account for the capacitance-frequency dispersion (see, e.g., description of SILENSE package[23]). Very roughly, the concentrations of the centers located in the QWs can be estimated using as a normalizing steady-state capacitance C in $\Delta C/C$, the capacitance corresponding to the chosen QW, and multiplying it by the average charge density in the QW. This, however, is at best an order of magnitude estimate. However, if, as with our studies of aging effects, the concentration profiles are not strongly affected, the ratio of the magnitudes of the peaks in DLTS or ODLTS before and after aging is reflecting the change in the concentrations of centers.

To assess the origin of the states causing the observed frequency dispersion of capacitance, we compared the defects observed in admittance spectra on various types of green LEDs. We commonly observe the presence of states with activation energies 0.077 eV, 0.13 eV, 0.27 eV,[20,24] 0.025 eV, 0.12 eV, and 0.2 eV.[19] The common features are the presence of states with activation energies 0.12–0.14 eV and 0.2–0.27 eV. The 0.025 eV and 0.07–0.08 eV states and the states similar to the 0.12–0.14 eV feature have been observed in blue LEDs of different designs.[10,11] The 0.12–0.14 eV level is attributed to freeze out of Mg acceptors, although it is not clear why the energy of such a transition would be dependent on applied bias, as shown in Fig. 1(c). Such a dependence is usually a manifestation of the Poole–Frenkel effect, due to the presence of high electric field, which should not be the case for acceptors in the heavily doped p-type layer of a p–n junction. Thus, the states that seem to be specific for green MQW structures are the ones with an activation energy of 0.2–0.27 eV. The high density of these states is responsible for the early capacitance–frequency roll-off in the diodes studied here, in contrast to green LEDs.[19,20,24] It is not likely that the difference in capacitance–frequency dispersion with temperature comes from the difference in contribution of quantized state in the QWs. This makes it probable that these states are of defect nature, as possibly are the shallower states with energies near 0.08 eV. The most likely place for defect states is the GaN/InGaN interface in the QWs.

IV. CONCLUSIONS

Green LEDs display strong temperature dependence of capacitance and AC conductance, regulated by the presence of deep states with ionization energies ~0.09 eV, 0.15 eV, and 0.3 eV at zero bias, with the first two showing dependence on the applied bias. These states lead to the concentration dependence on depth and on bias, because the states detected in admittance and some other deep states in the MQW region cannot follow the probing electric field. These appear to be related to defects in the QW, GaN barriers, or GaN/InGaN interfaces. The shift of C–V characteristics with temperature makes standard DLTS/ODLTS inaccurate. The remedy is to perform these at low frequency, with constant capacitance DLTS[17] or DLTS/ODLTS at low frequency with maintaining the LED capacitance between the DLTS/ODLTS relaxation curve measurement constant by varying the applied bias while keeping the temperature ramp slow (~2 K/min). This latter approach was used to detect a major electron trap at E_c–0.5 eV (electron trap A) and a major hole trap at E_v+0.6 eV (hole trap B) in the four GaN/InGaN QWs. Hole traps in the first set of QWs could be characterized by ODLTS with excitation photon energies higher than the QWs' InGaN bandgap, while the electron traps A in the QWs inside the SCR could be detected by ODLTS with excitation with subbandgap light (660 nm). The concentration of the A electron traps was the highest in the deepest QWs and decreased toward the p–n junction. The electron and the hole trap densities increased as a result of aging test carried out for 2120 h. However, the EQE of these green LEDs slightly increased after such tests, suggesting the main limitation to EQE comes from the presence of disordered local regions with lower effective bandgap. The origin of states with long-wavelength emission and low EQE may be due to localized regions with increased In concentration, but poor compositional uniformity, giving rise to low radiative recombination efficiency. The results show admittance/DLTS characterization of green GaN/InGaN MQW LEDs requires optimization.

ACKNOWLEDGMENTS

The work at NUST MISiS was supported in part by the Ministry of Education and Science of the Russian Federation in the framework of Increase Competitiveness Program of NUST (MISiS) (No. K2-2017-068). The work at Korea University was supported by the Technology Innovation Program (No. 20000261) funded by the Ministry of Trade, Industry & Energy (MOTIE, Korea). The authors thank Dr. S. Yu. Karpov for fruitful discussions.

REFERENCES

[1]S. H. Oh, B. P. Yonkee, M. Cantore, R. M. Farrell, J. S. Speck, S. Nakamura, and S. P. DenBaars, Appl. Phys. Express **9**, 102102 (2016).
[2]L. Jun-Lin, Z. Jian-Li, W. G.-Xu, M. Chun-Lan, X. Long-Quan, D. Jie, Q. Zhi-Jue, W. Xiao-Lan, P. Shuan, Z. Chang-Da, W. Xiao-Ming, F. Wen-Qing, and J. Feng-Yi, Chin. Phys. B **24**, 067804 (2015); J. H. Park, J. Cho, E. F. Schubert, and J. K. Kim, Energies **10**, 1277 (2017); Z. Lin, H. Wang, Y. Lin, M. Yang, W. Wang, and G. Li, J. Phys. D **49**, 115112 (2016); L. Wang, J. Jin, C. Mi, Z. Hao, Y. Luo, C. Sun, Y. Han, B. Xiong, J. Wang, and H. Li, Materials **10**, 1233 (2017); J. Piprek, Appl. Phys. Lett. **107**, 031101 (2015).

[3]M. Kneissl, "A brief review of III-nitride UV emitter technologies and their applications," in *III-Nitride UV Emitters*, edited by M. Kneissl and J. Rass (Springer, Switzerland, 2016), Chap. 1.
[4]H. Zhao, G. Liu, J. Zhang, R. A. Arif, and N. Tansu, J. Display Technol. **9**, 212 (2013).
[5]F. Nippert, S. Y. Karpov, G. Callsen, B. Galler, T. Kure, C. Nenstiel, M. R. Wagner, M. Straßburg, H.-J. Lugauer, and A. Hoffmann, Appl. Phys. Lett. **109**, 161103 (2016).
[6]S. Y. Karpov, Photonics Res. **5**, A7 (2017).
[7]C. M. Jones, C.-H. Teng, Q. Yan, P.-C. Ku, and E. Kioupakis, Appl. Phys. Lett. **111**, 113501 (2017).
[8]G. M. Martin, A. Mitonneau, D. Pons, A. Mircea, and D. W. Woodard, J. Phys. C Solid State Phys. **13**, 3855 (1980).
[9]A. Armstrong, T. A. Henry, D. D. Koleske, M. H. Crawford, K. R. Westlake, and S. R. Lee, Appl. Phys. Lett. **101**, 162102 (2012).
[10]A. Y. Polyakov, N. B. Smirnov, I. V. Shchemerov, E. B. Yakimov, E. E. Yakimov, K. C. Kim, and I.-H. Lee, ECS J. Solid State Sci. Technol. **7**, Q80 (2018).
[11]A. Y. Polyakov, N. B. Smirnov, E. B. Yakimov, H.-S. Cho, J. H. Baek, A. V. Turutin, I. V. Shemerov, E. S. Kondratyev, and I.-H. Lee, ECS Solid State Sci. Technol. **5**, Q274 (2016).
[12]I.-H. Lee, A. Y. Polyakov, S.-M. Hwang, N. M. Shmidt, E. I. Shabunina, N. A. Tal'nishnih, N. B. Smirnov, I. V. Shchemerov, R. A. Zinovyev, S. A. Tarelkin, and S. J. Pearton, Appl. Phys. Lett. **111**, 062103 (2017).
[13]I. H. Ho and G. B. Stringfellow, Appl. Phys. Lett. **69**, 2701 (1996).
[14]G. B. Stringfellow, J. Cryst. Growth **312**, 735 (2010).
[15]J. L. Pautrat, B. Katircioglu, N. Magnea, D. Bensahel, J. C. Pfister, and L. Revoil, Solid State Electron. **23**(11), 1159–1169 (1980).
[16]A. Y. Polyakov, N. B. Smirnov, I.-H. Lee, and S. J. Pearton, J. Vac. Sci. Technol. B **33**, 061203 (2015).
[17]D. K. Schroder, *Semiconductor Materials and Device Characterization* (John Wiley and Sons, New York, 1990), Chap. 7.
[18]A. Y. Polyakov, N. B. Smirnov, A. V. Turutin, I. V. Shemerov, F. Ren, S. J. Pearton, and J. W. Johnson, J. Vac. Sci. Technol. B **34**, 041216 (2016).
[19]A. Y. Polyakov, N. M. Shmidt, N. B. Smirnov, I. V. Shchemerov, E. I. Shabunina, N. A. Tal'nishnih, P. B. Lagov, Y. S. Pavlov, L. A. Alexanyan, and S. J. Pearton, ECS J. Solid State Sci. Technol. **7**, P323 (2018).
[20]I.-H. Lee, A. Y. Polyakov, N. B. Smirnov, I. V. Shchemerov, T.-H. Chung, P. B. Lagov, R. A. Zinov'ev, and S. J. Pearton, ECS J. Solid State Sci. Technol. **6**, Q127 (2017).
[21]M. Kim, S. Choi, J.-H. Lee, C. Park, T.-H. Chung, J. H. Baek, and Y.-H. Cho, Sci. Rep. **7**, 42221 (2017).
[22]E. Kioupakis, Q. Yan, and C. G. Van de Walle, Appl. Phys. Lett. **101**, 231107 (2012).
[23]See http://www.str-soft.com/products/SiLENSe/index.htm for details on effect of polarization on the properties of quantum wells used in light-emitting diodes.
[24]I.-H. Lee, H.-S. Cho, K. B. Bae, A. Y. Polyakov, N. B. Smirnov, R. A. Zinovyev, J. H. Baek, T.-H. Chung, I. V. Shchemerov, E. S. Kondratyev, and S. J. Pearton, J. Appl. Phys. **121**, 045108 (2017).